NUCLEAR SURFACE COMPLEX AS OBSERVED WITH THE HIGH RESOLUTION SCANNING ELECTRON MICROSCOPE

Visualization of the Membrane Surfaces of the Nuclear Envelope and the Nuclear Cortex from *Xenopus laevis* Oocytes

GERALD SCHATTEN and MARILYN THOMAN

From the Department of Biological Science, The Florida State University, Tallahassee, Florida 32306, and the Department of Molecular Biology, University of California, Berkeley, California 94720

ABSTRACT

The nuclear envelope and associated structures from *Xenopus laevis* oocytes (stage VI) have been examined with the high resolution scanning electron microscope (SEM). The features of the inner and outer surfaces of the nuclear surface complex were revealed by manual isolation, whereas the membranes facing the perinuclear space (the space between the inner and outer nuclear membranes) were observed by fracturing the nuclear envelope in this plane and splaying the corresponding regions apart. Pore complexes were observed on all four membrane surfaces of this double-membraned structure. The densely packed pore complexes ($55/\mu m^2$) are often clustered into triplets with shared walls (outer diameter = 90 nm; inner diameter = 25 nm; wall thickness = ~30 nm), and project ~20 nm above each membrane except where they are flush with the innermost surface. The pore complex appears to be an aggregate of four 30-nm subunits. The nuclear cortex, a fibrous layer (300 nm thickness) associated with the inner surface of the nuclear envelope, has been revealed by rapid fixation. This cortical layer is interrupted by funnel-shaped intranuclear channels (120–640 nm diam) which narrow towards the pore complexes. Chains of particles, arranged in spirals, are inserted into these intranuclear channels. The fibers associated with the innermost face of the nuclear envelope can be extracted with 0.6 M KI to reveal the pore complexes. A model of the nuclear surface complex, compiled from the visualization of all the membrane faces and the nuclear cortex, demonstrates relations between the intranuclear channels ($3.2/\mu m^2$) and the numerous pore complexes, and the possibility of their role in nucleocytoplasmic interactions.

KEY WORDS nuclear envelope · nuclear cortex · scanning electron microscopy · nuclear membrane · nuclear pore complex · intranuclear channel · nucleo-cytoplasmic interactions

The positioning of the nuclear envelope between the sites of transcription and translation, and the unusual pore complexes of the envelope, make this structure a likely candidate for a role in processing and controlling the release of gene products (17, 22). The possible involvement of

the pore complex in this activity is especially interesting since the density of pore complexes per nucleus can be correlated with genetic activities (34). However, in the absence of evidence regarding the function of the nuclear envelope, biochemical characterizations and morphological descriptions may provide some insights into its biological properties.

The sources of knowledge concerning the nuclear envelope can be grouped into the following basic categories: biochemical analyses after nuclear envelope isolation (reviewed in reference 28); transmission electron microscope (TEM) observations of the nuclear envelope (reviewed in references 17, 20, and 47) and of the pore complex (reviewed in reference 33); biophysical and permeability investigations (reviewed in references 13 and 30); and transplantation studies (reviewed in reference 22). The TEM data have resulted in models of the nuclear envelope demonstrating a great complexity (1, 9, 12, 13, 17, 47 and 49). The scanning electron microscope (SEM) observations presented here confirm and extend the complexity of the nuclear envelope and of surface-associated structures.

Recently developed techniques for the isolation of the nuclear envelope (28) and the nuclear pore complex-lamina (1) have provided detailed information concerning the chemical composition of the nuclear envelope and associated structures: the nuclear surface complex. Additionally, these isolation techniques have been exploited by electron microscopists in conjunction with negative staining to complement descriptions of the nuclear envelope obtained by thin section (45) and information obtained by freeze-fracture and -etch techniques (26). High resolution SEM of the outer surface of isolated mouse liver nuclei has augmented the utility of this instrument in providing topographical information about the ultrastructure of the nuclear surface and the pore complex (29). In that work, comparisons of the SEM images with specimens processed for the TEM confirmed the parity of dimensions and structural relations in both microscopes.

SEM techniques for examining the inner surface of the cell membrane and structures associated with it have been developed (6, 48), and reconstructions of the inner and outer faces of the cell surface have been compiled (42). In this report, the nuclear envelope was subjected to a similar scrutiny, i.e., the inner and outer faces were examined and a reconstruction was made. The giant germinal vesicle from *Xenopus laevis* oocytes was manually isolated to avoid the distortions of centrifugation and lengthy homogenization procedures required for isolation of nuclei from most other cells. The inner and outer features of the nuclear envelope were revealed by simply tearing the nucleus open. Visualization of the surfaces facing the region between the inner and outer nuclear membranes, i.e., facing the perinuclear space, was possible only after fixation of the whole oocyte in osmium tetroxide and critical point drying. The dry egg, when cracked, fractured in the plane between the two nuclear membranes, which then permitted observations of these membrane surfaces. The nuclear cortex, a fibrous layer associated with the inner face of the nuclear envelope, is quite labile and is best preserved by rapid glutaraldehyde fixation. The images of both faces of each nuclear membrane, and of this fibrous region, in conjunction with the known TEM data, have been compiled to produce a schematic model of the nuclear surface complex from the *Xenopus* germinal vesicle, and perhaps a model of the nuclear envelope generally.

MATERIALS AND METHODS

Xenopus Rearing

Xenopus laevis, 150–200 g, were obtained from the South African Snake Farm (Fish Hoek, South Africa), and maintained in bathtubs of tap water at 18–22°C. Animals were fed twice weekly on beef heart. Frogs were injected with 100 U of pregnant mare serum gonadotrophin (obtained from the Rat Pituitary Hormone Distribution Program, NIAMDD) 3–7 days before use.

Ovarian tissue was removed through an incision in the dorsal body wall from frogs anesthetized for 45 min in 0.15% tricaine (*p*-methyl benzene sulfonate sodium salt, Calbiochem, San Diego, Calif.), pH 6.8, in tap water. The ovary was washed in Modified Barth's Solution (MBS),[1] cut into pieces ~1 cm^2, and transferred to fresh MBS.

Oocytes (stage VI, 1.25–1.4 mm) were dissected from their ovarian follicles with watchmaker's forceps and stored at room temperature in MBS until use.

Nuclear Isolation

Oocytes were transferred from the MBS to a medium composed of 150 mM KCl, 5 mM Tris, 1 mM $MgCl_2$, pH 7.8 (hereafter called isolation medium). The nuclei were isolated in this solution by splitting the oocyte at

[1] 88 mM NaCl, 1 mM KCl, 0.82 mM $MgSO_4$, 0.33 mM $Ca(NO_3)_2$, 0.41 mM $CaCl_2$, 2.4 mM $NaHCO_3$, 1.5 mM Tris·HCl, pH 7.8.

the animal pole with fine-tip forceps, and subsequently applying pressure to the sides of the cell (5). The resultant pressure forced the germinal vesicle through the split surface at the animal pole. The isolated nuclei were washed free of adhering yolk by drawing them in and out of a wide-bore Pasteur pipette.

Preparation of the Isolated Nuclear Envelope

The clean nuclei in the isolation medium were allowed to settle onto a glass surface which had been previously coated with polylysine (36). After the nucleus affixed to this substrate, it was opened manually by tearing with forceps. This tearing resulted in the release of the nuclear sap and chromatin as an opalescent coagulum. Invariably the remaining nuclear envelope was folded at the periphery which permitted simultaneous observations of both the inner and outer faces of the nuclear envelope, as in Fig. 1. The slide with the attached and opened nuclear envelope was placed in a fixative solution of 2.5% glutaraldehyde in the isolation medium at pH 7.8, for 30 min. These samples permitted observations of the outer and the inner surfaces of the nuclear envelope.

Splitting of the Nuclear Envelope to Expose the Surface of Each Nuclear Membrane Facing the Perinuclear Space

Whole oocytes were fixed overnight at room temperature in 1% OsO_4, and postfixed in 2.5% glutaraldehyde for 1 h. The oocytes were dehydrated in ethanol, infiltrated with Freon TC, and dried at the critical point in Freon 13. The dry oocytes were attached to double-sided tape and cracked in half with the tips of microfor-

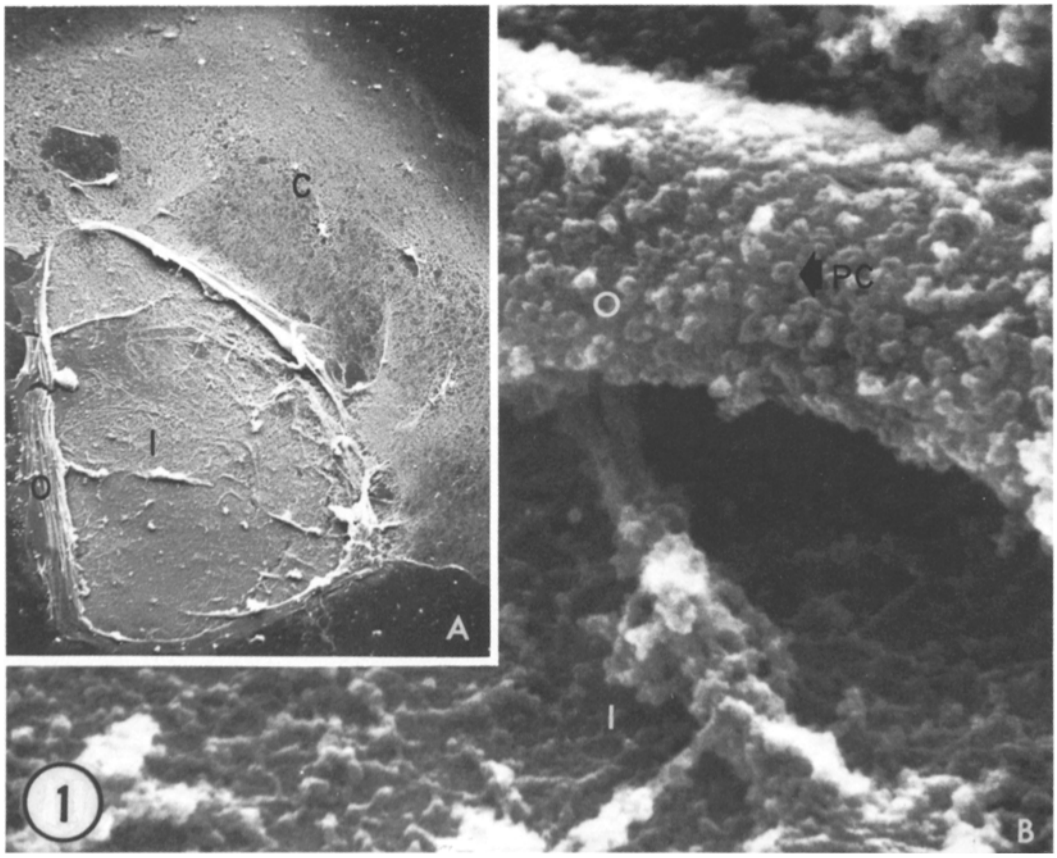

FIGURE 1 (A) A manually isolated nuclear envelope which had been torn open with microforceps. In this preparation, which is attached to a polylysine-coated glass slide, the inner surface of the nuclear envelope (*I*) is apparent in the center of the image. The outer surface (*O*) is viewable in the folded regions at the periphery. Chromatin (*C*) remained attached in this preparation and can be observed to adhere to the plate. × 150. (B) A folded region of the nuclear envelope. The pore complexes (*PC*) can be seen projecting from the outer surface (*O*), whereas the inner surface (*I*) is covered by fibrous material. × 28,000.

ceps. This cracking procedure usually revealed the nucleus with a portion of the nuclear envelope split in the plane of the perinuclear space (see Fig. 4). The egg fragments were gently splayed open for proper orientation in the SEM (Figs. 5 and 7). Examinations of the surfaces of both membranes of the nuclear envelope were performed in such samples. Subsequent experiments have demonstrated that 1% OsO_4 alone without the glutaraldehyde postfixation is sufficient for fracture in the perinuclear plane.

Fixation of the Nuclear Cortex

The nuclear cortex seems to be quite labile, as others have noted (12, 40), and is best preserved with a glutaraldehyde fixation. The most favorable results were obtained when live oocytes were rapidly torn open upon being immersed into 2.5% glutaraldehyde in the isolation medium. The tearing step is somewhat random, but often the nucleus is exposed as in Fig. 12, which permits studies of the substructure associated with the inner surface of the nuclear envelope.

Processing Procedure

After fixation, all specimens were dehydrated in ethanol, infiltrated in Freon TC, and dried at the critical point in Freon 13. The samples were coated with about 80 Å of platinum-carbon on a rotating stage and examined in a field emission SEM with an accelerating voltage between 14.5 and 17 kV.

RESULTS

Outer Surface of Nuclear Envelope

An isolated germinal vesicle manually torn open after attachment to a polylysine-coated glass slide is shown in Fig. 1*A*. The outer surface of the nuclear envelope adheres tenaciously to the positively charged substrate. The inner surface of the nuclear envelope is exposed in the center of this preparation, while the folded regions at the periphery permit observations of the outer surface of the nuclear envelope. Infrequently, chromatin remains associated with the opened nucleus, and it is observed in this preparation at the upper right as a netting of fibrous material which also adheres to the polylysine coating.

A folded region at higher magnification is depected in Fig. 1*B*. In such preparations, both the inner and outer faces of this structure can be examined simultaneously. The inner surface of the isolated preparation will be described in a later section. The outer surface is characterized by the dense packing of the pore complexes, and there are ~58 pore complexes/μm^2, which agrees well with other published data (16). These pore complexes project ~20 nm above the membrane surface and have indentations suggesting a hollow channel as observed in the TEM (33). In regions where the nuclear envelope is folded, the pore complexes follow the contour of the nuclear envelope rather than appearing like stiff insertions in the membrane. Pore complexes often appear to share outer walls forming triplet clusters (arrows, Fig. 2). The outer diameter of the pore complexes measures 90 nm, the inner 25 nm, while the wall thickness is ~30 nm. The pore complex often appears as an aggregate of four rectangularly arranged particles which circumscribe an opening (Fig. 3, arrow; see Table I). These particles are ~30 nm in diameter. Occasionally, there are holes in the membrane which might be a drying artifact in the preparation of this material. Treatments with detergents, or the absence of divalent cations in the isolation media, increase the number of these holes, resulting in pore complexes connected to one another by fibers as previously reported by Scheer et al. (44). Crescent-shaped mitochondria were, at times, found associated with the nuclear envelope, as has been previously reported (18). However, there was no evidence of the association between the nuclear envelope and other intracellular organelles such as the endoplasmic reticulum.

The image of the outer surface of the nuclear envelope in this work does not differ much from that obtained using shadowed replicas of air-dried, isolated envelopes (15) or that described in other published reports on negative staining of isolated envelopes (5, 9, 38) or on thin-section and freeze-fracture studies of cells or isolated material (see references 17 and 33).

Membrane Surfaces Facing Perinuclear Space

When whole oocytes are fixed, dried at the critical point, and cracked open in this dry state, the nuclear envelope almost invariably splits in the plane between the inner and outer nuclear membranes. Observations are then permitted of the surfaces which face the perinuclear space, allowing the study of corresponding regions on the inner and outer nuclear envelopes. Fig. 4 schematically indicates the fracture plane with these dried, cracked egg fragments. The lightly stippled outer nuclear membrane has remained attached to the right half (as in Figs. 7 and 8) while the corresponding region of the inner nuclear membrane (darkly stippled in Fig. 4) is observed in Figs. 5, 6, and 9 where this surface has been

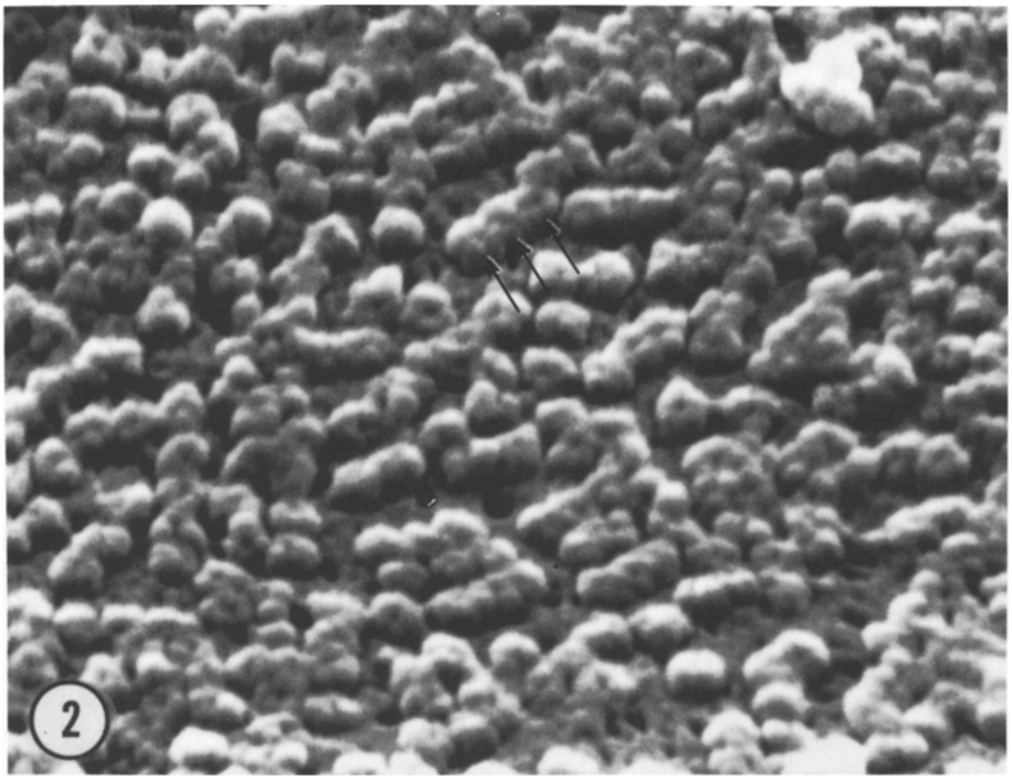

FIGURE 2 The outermost surface of the nuclear envelope is characterized by a dense packing of the projecting nuclear pore complexes. The pore complexes are often clustered to form triplets in which the common walls are shared (triple arrow). × 65,000.

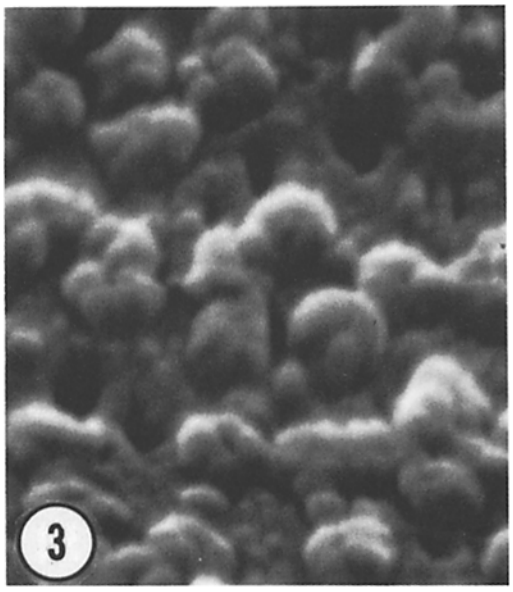

FIGURE 3 The tetrameric nature of the pore complex is apparent in this high magnification of the outer surface of the nuclear envelope. This is best observed in the pore complexes at the top and bottom of the image. With the magnifying abilities of the SEM, it is demonstrated that the pore complex appears on the outer surface as an aggregate of four components. × 100,000.

exposed. The terminology used here will refer to the face of the respective nuclear membrane. For instance, the lightly stippled region on the right is the inner face of the outer nuclear membrane, whereas the darkly stippled area on the left is the outer face of the inner nuclear membrane.

Figs. 5 and 7 are images of an oocyte split to reveal the membrane surfaces facing the perinuclear space. These images have been positioned on opposing pages so that superimposition of corresponding areas is possible by closing the journal. In Fig. 5, the nucleus can be observed as the spherical area in the yolk-filled cytoplasm. Near the animal pole of this nucleus, there is a patch of the nuclear envelope (arrow). This patch is the surface of the inner nuclear membrane that faces the perinuclear space. The chromatin can be

TABLE I

Frequency of Subunits in Nuclear Pore Complexes

No. of subunits/pore complex	%
3	3.3
4	91.8
5	4.9

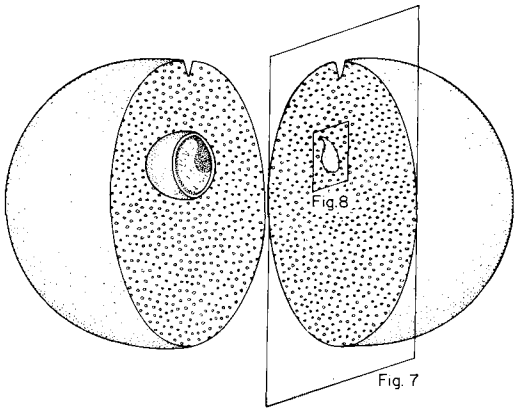

FIGURE 4 This schematic diagram depicts the fracture plane resulting in the exposure of the membrane surfaces facing the perinuclear space. The fixed and dried oocyte was cracked by inserting microforceps (indentation at top). The left half is diagrammatic of Figs. 5, 6, and 9, whereas the right half, as framed in this schematic drawing, corresponds to Figs. 7 and 8. The lightly stippled outer nuclear membrane remained adhered to the right half, as in Fig. 8. The removal of the outer membrane from the right half resulted in the exposure of the inner nuclear membrane (darkly stippled), as in Fig. 6 in the left half. The terminology used throughout this report will refer to the darkly stippled region on the left as the outer face of the inner nuclear membrane, and the lightly stippled area on the right as the inner face of the outer nuclear membrane.

observed beneath this patch, filling the nucleus.

The corresponding half of this cracked oocyte is visualized in Fig. 7. The indentation at the top of this cell resulted from the insertion of the microforceps used in the cracking procedure. Just beneath this indentation, the patch of nuclear envelope corresponding to that observed in Fig. 5 can be seen (arrow). This is the surface of the outer nuclear membrane that faces the perinuclear space.

Figs. 6 and 8 are higher magnifications of the nuclear membranes visualized in Figs. 5 and 7, respectively. In Fig. 6, there are four clearly apparent protrusions (mean diameter = 5.75 μm) which are perhaps nucleoli protruding from within the nucleus. Chromatin can be observed to the left of this membrane patch, where the nuclear interior is exposed. Close examination of the surface will reveal hollow projecting pore complexes which have the same outer diameter as those observed on the outer surface (i.e. 90 nm; arrow). It is significant that there are, again, pore complexes with fused walls, commonly in groups of three (arrow).

The surface of the outer nuclear membrane that faces the perinuclear space is shown in Fig. 8. The four depressions match the protrusions observed in Fig. 6; pore complexes ($\sim$55/μm^2) and sets of fused pore complexes also correspond. That these two membrane faces are corresponding areas can be vividly demonstrated by superimposing the images upon one another. As with Figs. 5 and 7, this can be done by closing the journal. Unfortunately, it is not possible to obtain clear photographs of these preparations at very high magnifications, probably because of the vibration of the large egg fragment which has only limited areas of attachment to the double stick tape. Fig. 9 is a higher magnification image where the pore complexes can be observed. The relative density of the pore complexes over the protrusions, which might be nucleoli, and over the flat areas on the nuclear membrane are about the same, indicating that there does not seem to be any preferential placement of these structures. Interestingly, the membrane surfaces facing the perinuclear space are covered with coarse particles $\sim$20 nm, which do not seem to appear on the inner and outer faces of the nuclear envelope.

Inner Surface of Nuclear Envelope

The isolated nucleus, when torn open as in Fig. 1, permits observations of the inner surface of the nuclear envelope. This surface appears as a fibrous network (fiber diameter down to 15 nm) overlaid by particles of 50–60 nm (Fig. 10). Chromatin strands, which can be distinguished from the fibrous network by their characteristic beaded appearance, are occasionally found associated with the inner surface of the nuclear envelope. The fibrous matrix is interrupted by holes with diameters approaching 25 nm, i.e. the diameter of pore complexes. The density of these interrupting holes is $\sim$55/μm^2, a value that is consistent with the density of pore complexes observed on all other membrane faces.

It is not possible to discern whether the holes

are pore complexes in this preparation, or whether they are merely spaces circumscribed by the fibers associated with the inner surface of the nuclear envelope. The fibers can be extracted by rinsing the isolated nuclear envelope in 0.6 M KI for 5 min and then processing as usual. This treatment extracts all the fibers associated with the inner surface of the nuclear envelope, thereby permitting direct observation of the inner face of the inner nuclear membrane (Fig. 11).

The pore complexes that can be observed in these preparations have the same size and density as those observed on the outer surface of the nuclear envelope (60/μm^2). The pore complexes do not project as much above the membrane face on this surface as they do on the outer surface of the nuclear envelope and on the membrane surfaces facing the perinuclear space, where the pores protrude from the membrane surface by ~20 nm. It is also significant that there are fused pores, again three to a group (arrow).

The Nuclear Cortex

When oocytes are rapidly torn open after being plunged into the glutaraldehyde fixative, the nucleus is often exposed. Such a preparation is shown in Fig. 12. The nucleoplasm is generally lost after this treatment, implying only a tenuous connection between the chromatin and the nuclear envelope at this stage (44). Observations are then permitted of the substructure associated with the inner surface of the nuclear envelope.

When chromatin remains attached to the nuclear envelope, it is often associated with the vegetal pole of the nucleus (as determined by the size of the yolk platelets adjacent to the nucleus). The chromatin appears as beaded strands with a diameter of 40–100 nm. When stereo images are analyzed, the spiral arrangement of the beads is apparent. Chromatin fibers are depicted in Fig. 10 (at *C*) and in Fig. 13. Interestingly, there is a modification at the site of chromatin attachment to the nuclear envelope (Fig. 13, arrow). This modification appears as an invagination of the nuclear envelope, with the chromatin strands radiating from this site. Unfortunately, the drying procedure required for scanning electron microscopy cannot exclude the possibility of the collapse of these structures.

The ultrastructure of the inner surface of the nuclear envelope in these rapidly fixed specimens is considerably different from that seen in the isolated nuclear envelopes or in those cracked open after fixation. The torn regions at the periphery permit measurements of the thickness of the nuclear envelope (~300 nm). Large, flattened circles 0.45 μm in diameter, possibly collapsed nucleoli, are attached to the envelope (Fig. 14). Careful examination of the inner surface of the nuclear envelope prepared this way reveals that it is covered by a substructure that has not been reported previously. At this magnification, there is the impression of a complete fibrous layer covering the inner surface, with a second, incomplete layer covering the first layer.

A higher magnification image of this structure (Fig. 15) demonstrates that the entire inner surface of the nuclear envelope is covered by fibers which overlap to circumscribe funnels, called intranuclear channels by Watson (49). The intranuclear channels in this image are of varying inner diameters (120–640 nm) and often have chains of particles inserted within them (arrow). These particles are ~50–60 nm in diameter and may be analogous to the spirals of ribonucleic acid-protein aggregates associated with the nuclear pore reported in other systems (41, 50).

Fig. 16 demonstrates that the intranuclear channels open at the nucleoplasmic surface and narrow towards the nuclear envelope. This narrowing is accomplished by the successive diminution of the diameter circumscribed by the fibers. The smallest diameters measured approach that of the 25-nm lumen of the pore complex. The chains of particles and individual particles are apparent in this image, and again are associated with the open end of the intranuclear channel. There are ~3.2 intranuclear channels per μm^2, considerably fewer than the number of pore complexes. The several ways of explaining the discrepancy between the number of intranuclear channels and the number of pore complexes are stated in the Discussion and in Fig. 17.

DISCUSSION

Model of the Nuclear Surface Complex

The images of the faces of each membrane of the nuclear envelope, as well as the fibrous layer associated with the nuclear envelope which we shall call the nuclear cortex, have been compiled to reconstruct a three-dimensional model of the nuclear surface complex of the *Xenopus* oocyte. This schematic model does not differ greatly from other proposed models of the pore complexes and of the nuclear envelope (1, 9, 12, 13, 17, 47 and

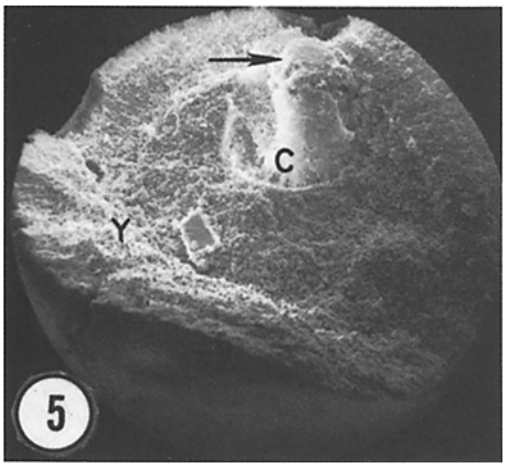

FIGURE 5 An oocyte split to reveal the outer face of the inner nuclear membrane. Refer to Fig. 4 and compare this image with Fig. 7. The oocyte was fixed with osmium tetroxide, dehydrated, dried at the critical point, and fractured with the tips of microforceps (indentation at top of oocyte). The fracture plane, after this drying procedure, is the perinuclear space, thereby exposing the inner face of the outer nuclear membrane (Figs. 7 and 8) and the outer face of the inner nuclear membrane (Figs. 5, 6, and 9). The other half of this fractured oocyte is depicted in Fig. 7, and comparisons should be made by closing the journal to superimpose the areas of interest. The nucleus is observed in the center, and is filled with chromatin (*C*). The yolky cytoplasm (*Y*) is similarly apparent. At the top of the nucleus (arrow) is a patch of the split nuclear envelope. × 100.

49), but provides additional information regarding the appearance of the membrane surfaces, the geometry of the pore complexes and their associations with adjacent pore complexes, and the relationship between the nuclear cortex and the nuclear envelope.

The schematic model (Fig. 18) shows all four membrane faces of the nuclear envelope simultaneously, and the associated nuclear cortex. On the outermost face, the smooth membrane is studded with pore complexes which project from the level of the membrane. The pore complexes appear to be composed of four units, and often the pore complexes are fused into triplets which share adjoining walls. The inner and outer nuclear membranes are shown splayed apart in the diagram to reveal the surfaces facing the perinuclear space. The appearance of each of these membrane faces

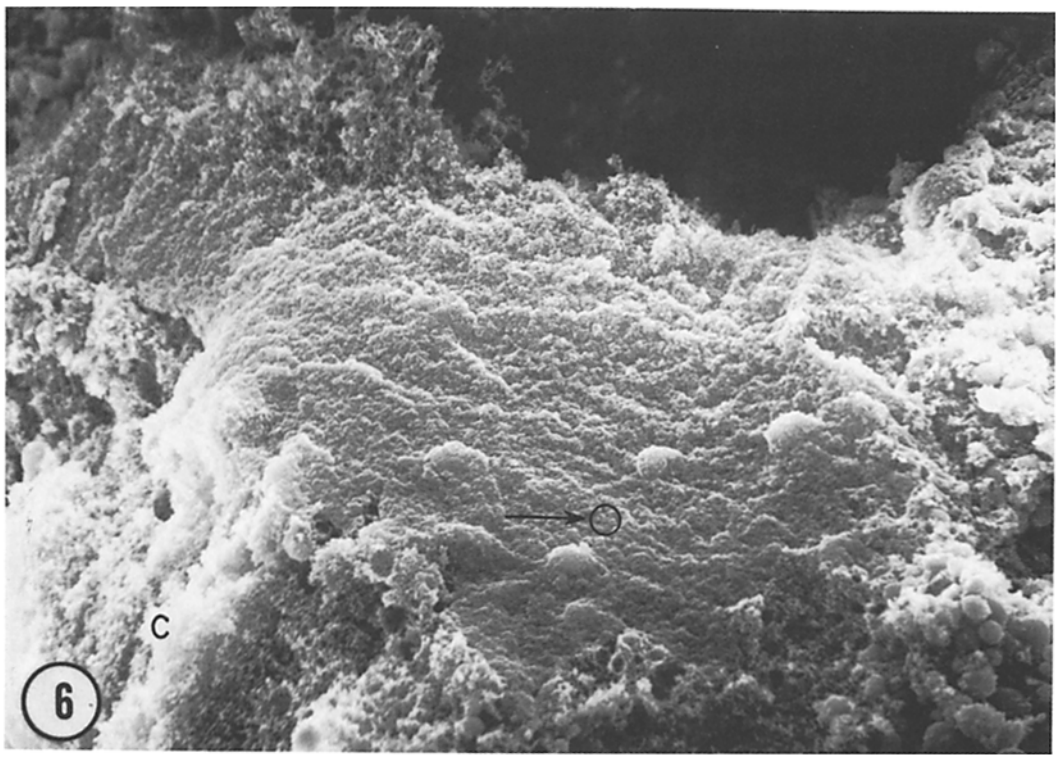

FIGURE 6 A higher magnification of the outer face of the inner nuclear membrane. Refer to Fig. 4 and compare with Fig. 8 for the corresponding region of the inner face of the outer nuclear membrane. A triplet of pore complexes has been circled and can be seen to coincide with those circled in Fig. 8. × 1,500.

is similar: a coarse, particle-covered membrane with pore complexes projecting from the surface. The pore complexes are fractured in the plane of the perinuclear space such that each membrane has half of the complex. This is demonstrated by superimposing images of the same region of the inner face of the outer nuclear membrane on images of the outer face of the inner nuclear membrane (as in Figs. 6 and 8). On the inner face of the inner nuclear membrane, the pore complexes do not seem to project much above the membrane surface. Furthermore, there are fibers covering this surface, which must be extracted before the pore complex can be observed. Associated with the inner surface of the nuclear envelope is a thick region of fibers that circumscribe funnels, the intranuclear channels. This substructure can be best preserved by rapid fixation, and probably represents the layer which in vivo accounts for the active or passive transport abilities of the nuclear envelope, as well as for the shape of the nucleus.

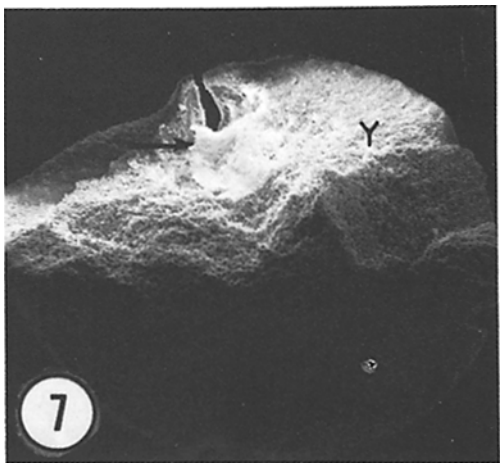

FIGURE 7 An oocyte split after drying revealing the inner face of the outer nuclear membrane (arrow). The complementary half of this oocyte is shown in Fig. 5. Refer to Fig. 4 for orientation. × 100.

Geometry of the Pore Complex

In this work, the pore complex is shown to be composed of an aggregate of particles projecting from all membrane faces, except for the innermost face. The density of the pore complexes on all membrane faces is about the same, indicating that there are no incomplete pores, and these results are consistent with the density (45) and sizes (33) observed in other work. Frequently, the pore

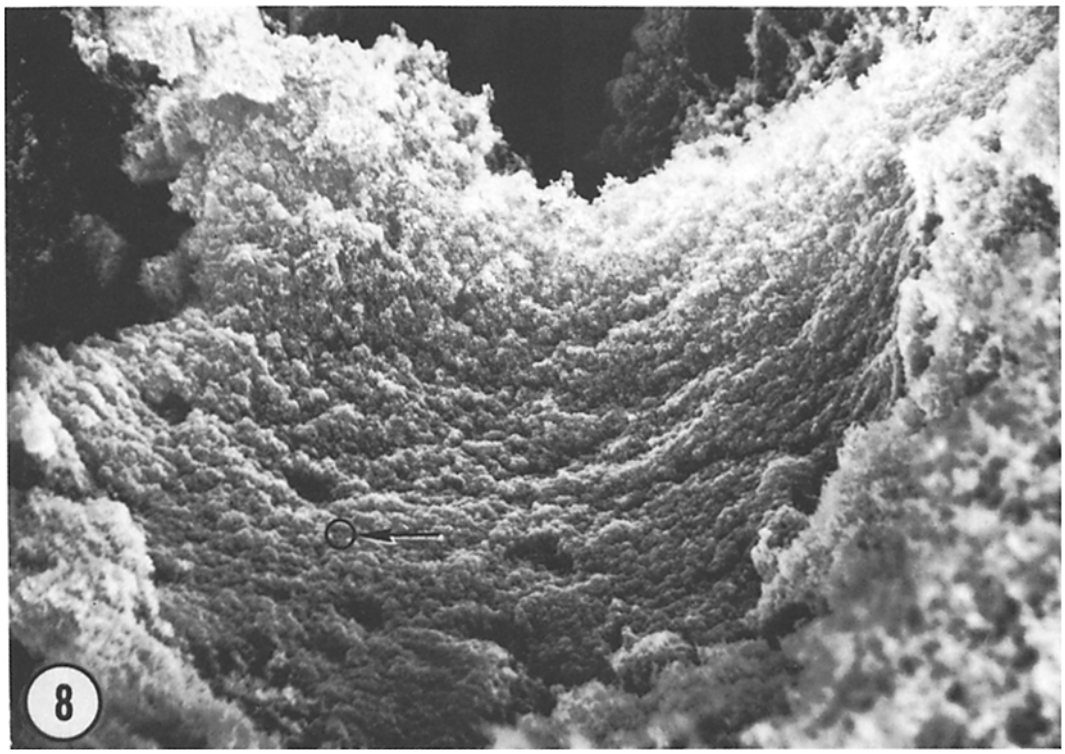

FIGURE 8 The inner face of the outer nuclear membrane. This magnified region of Fig. 7 corresponds to the area depicted in Fig. 6. Refer to Fig. 4 for orientation. The circled triplet of nuclear pore complexes will superimpose with that circled in Fig. 6. × 1,500.

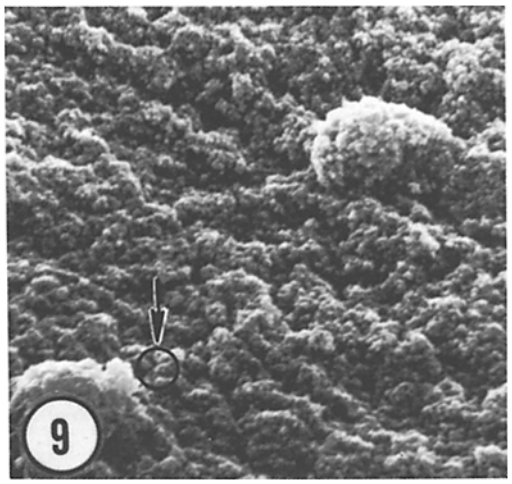

FIGURE 9 The outer face of the inner nuclear membrane. This image demonstrates the pore complexes and coarse nature of the membranes facing the perinuclear space. A triplet of pore complexes has been circled. The inner face of the outer nuclear membrane has a similar appearance. The limited attachment of the fractured oocyte to the adhesive tape results in sample vibration which does not permit high magnification photography. × 3,500.

complexes are fused, sharing adjoining walls to form triplets. These triplet structures have been observed on all membrane surfaces.

Each pore complex appears as an aggregate of four subunits in this work (see Table I) as in the work of Kirschner et al. (29). Although the evidence for the octagonal nature of the pore complex is excellent (11, 21, 32), those results were obtained with TEM. However, the octagonal arrangement of the pore complex need not necessarily be within a single membrane plane. In negative staining or thin sectioning, the TEM condenses a rather thick nuclear envelope or section into the single plane of the photographic image. This might possibly result in the superimposition of structures that are slightly out of plane with respect to one another. If this is the case, then the pore complex may actually be composed of two sets of four particles that are staggered at 90° from one another. Fabergé (10) arrived at the conclusion that the octagonal pore complex might well be composed of two sets of rectangularly arranged tetramers in staggered conformation. The limitation of the SEM in visualizing only surfaces might then result in the tetrameric appearance of the pore complex. However, the limited resolution of the SEM does not exclude the possibility that each particle is not a dimer. Until this can be clarified, a definite understanding of the morphology of the pore complex will not be possible.

Whenever the membranes of the nuclear envelope are split apart, the pore complex always fractures in the plane of the perinuclear space. Furthermore, half of each pore complex remains with each nuclear membrane. The pore complexes never seem to be pulled out of one membrane and left in the other, nor do there ever seem to be partially broken pore complexes with incomplete particle clusters in one membrane, with the missing particles in the other. This splitting of the pore complex within the perinuclear space implies that the complex has a natural cleavage plane in this region, or that it is composed of stacked particles rather than a solid cylinder, as proposed by Engelhardt and Pusa (9). In our reconstruction, the pore complex is shown to be the element responsible for maintaining the uniform separation between the two nuclear membranes. The nuclear membranes are also shown to be continuous, and they are torn when they are fractured apart. However, our evidence does not permit us to make conclusive statements about these points. For example, we cannot resolve the continuity of the two nuclear membranes nor can we be certain that the pore complex is solely responsible for the attachment of these membranes to one another. Furthermore, we cannot rule out the possibility that the pore complex between the inner and outer nuclear membranes is formed by these membranes. For instance, if the pore were created as a result of a cylindrical perforation where the inner and outer membranes meet, then when fractured and shadowed with platinum-carbon a structure with a wall diameter approaching 30 nm might possibly be observed.

Nuclear Cortex

The term nuclear cortex is used here to describe the fibrous layer associated with the inner surface of the nuclear envelope. This term has been chosen with analogy to the relations between the cell cortex and the plasma membrane, and those predicted to occur between the nuclear cortex and the nuclear membranes. A layer similar to the nuclear cortex has been described in many systems (2, 3, 7, 12, 14, 23, 25, 35, 38, 39, 46) by terms such as fibrous lamella (7, 12), internal dense lamella (46), zonula nucleum limitans or nuclear limiting zone (39), honeycomb layer (14), and

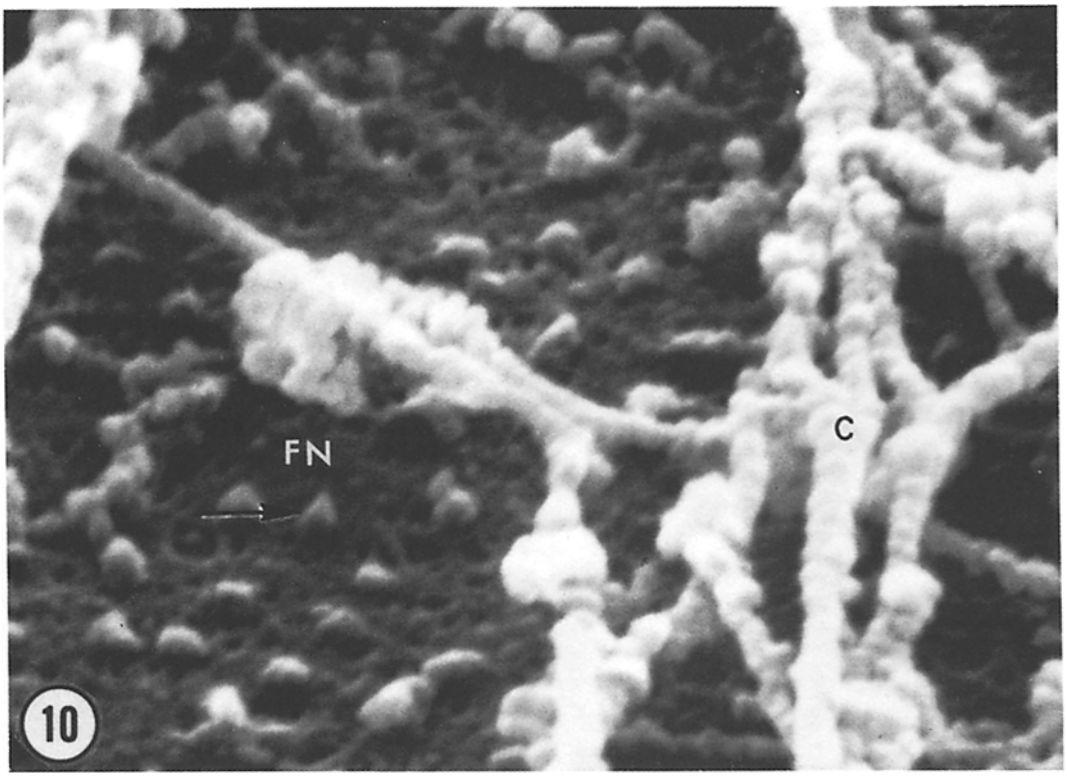

FIGURE 10 The inner surface of the isolated nuclear envelope. This image demonstrates the beaded nature of the chromatin strands (*C*) and reveals that the inner surface of the nuclear envelope after isolation appears as a fibrous network (*FN*) interrupted by holes. There are 50- to 60-nm particles (arrow) associated with this network. Pore complexes, which probably are covered by the fibrous network, are not apparent in these isolated preparations. × 65,000.

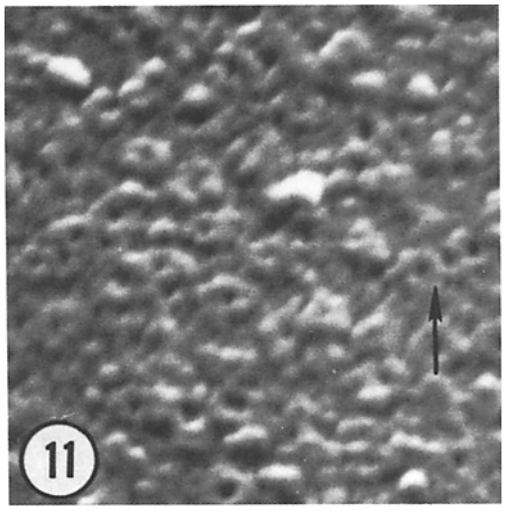

FIGURE 11 The inner surface of the isolated nuclear envelope after extraction with 0.6 M KI. After this extraction, the network and particles are removed from the inner surface, and pore complexes are apparent. These pore complexes, like those observed on the other three membrane surfaces, are found in a triplet array (arrow) but do not project above the membrane surface. × 65,000.

cortical nuclear layer (3). This terminology is used to simplify and clarify the vocabulary of this cellular structure; it is hoped that confusing and repetitive descriptive terms can be minimized. All the previous work on the nuclear cortex has been performed with thin sections for the TEM, revealing an electron-dense region underlying the inner surface of the nuclear envelope which is interrupted by electron-transparent areas adjacent to the pore complex. If a three-dimensional reconstruction of these sections were compiled, it would be predicted that the resultant image would not be unlike that obtained with the SEM: a thick matrix of fibers circumscribing funnel-form chan-

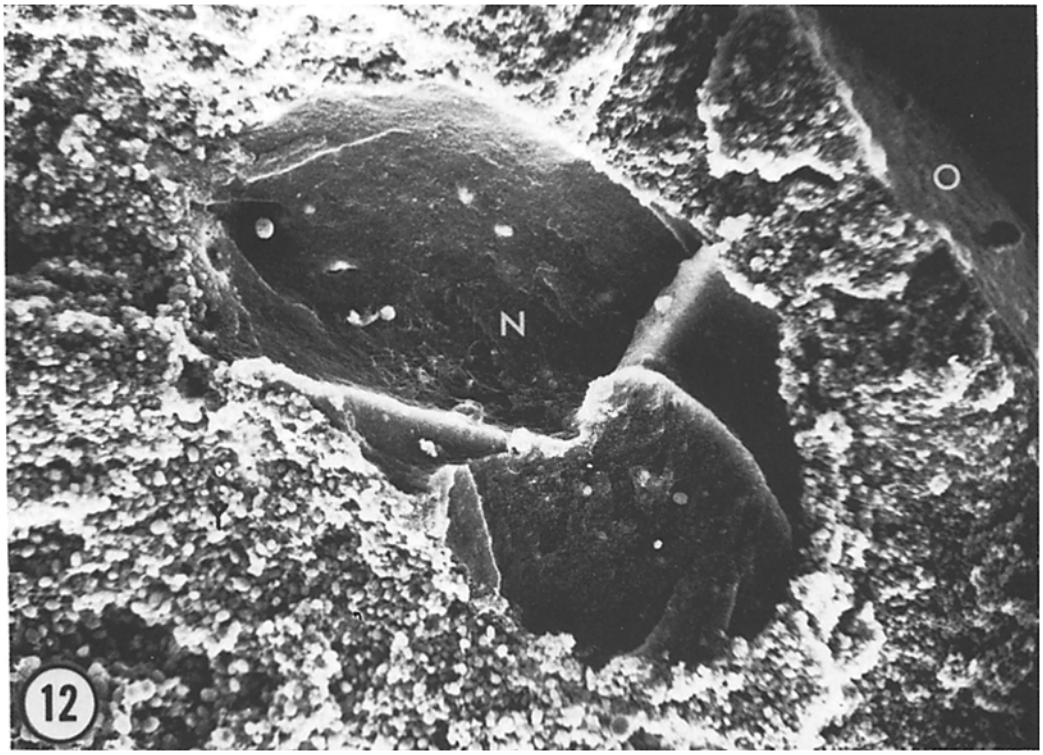

FIGURE 12 A rapidly fixed oocyte fragment prepared by ripping open the oocyte as it was plunged into glutaraldehyde. The nucleus (*N*) and the outer surface of the cell (*O*) can be observed. Rapid fixation was essential for the preservation of the nuclear cortex. × 325.

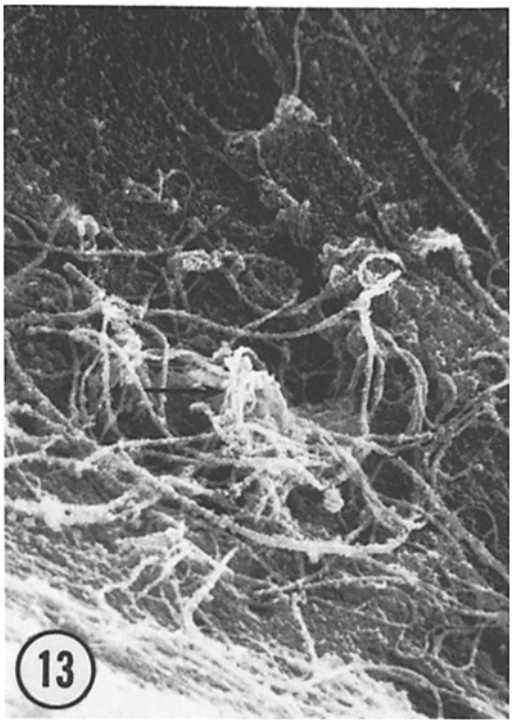

FIGURE 13 Chromatin attachment site. There is an invagination of the nuclear envelope, at the vegetal pole of these rapidly fixed oocytes, to which the chromatin seems to be attached (arrow). × 3,000.

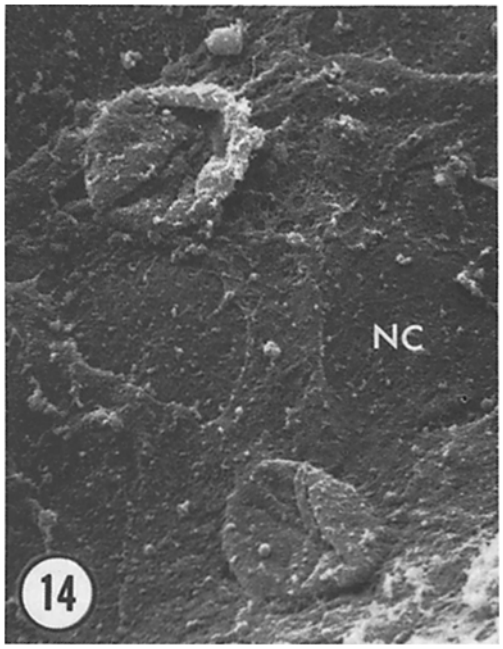

FIGURE 14 The inner surface of the nuclear envelope in a rapidly fixed oocyte. A layer covering the inner surface of the nuclear envelope, the nuclear cortex (*NC*), and large flattened structures, perhaps collapsed nucleoli, are observed in this preparation. × 2,000.

nels which, probably, lead to the orifices of the pore complexes.

It has not been possible to observe the geometry of the association between the intranuclear channels and the pore complex. The discrepancy between the density of intranuclear channels (3.2/μm^2) and the density of the pore complexes (~55/μm^2) can be reconciled by three possible modes of attachment (see Fig. 17): (*a*) The intranuclear channels might bifurcate towards the nuclear envelope. This would imply that a single intranuclear channel would service 18 pore complexes. The TEM evidence (e.g. references 12 and 24) does not confirm the existence of any bifurcations, so this possibility seems unlikely. (*b*) The intranuclear channels might terminate at a region close to, but not at, the pore complexes. Then, material might be deposited into this region and would sift to several pores at the same time. Were this the case, then isolation of nuclear envelopes associated with a lamina would not be predicted, so this possibility also seems improbable. (*c*) The channel might lead directly to a pore complex, as has been observed in thin section and after isolation. The material funneled into the intranuclear channel would be directly transported through the connecting pore complex. The possible connection of a single channel to a single pore complex does not exclude the breaking of that connection after some activity has occurred, and then the immediate reformation of that channel with another pore complex.

The chains of particles inserted within the intranuclear channels have been described in TEM work (41, 49) and appear to be composed of ribonucleoprotein complexes as determined by high resolution autoradiography (50). Their role in gene expression and in nucleocytoplasmic transport might prove profound.

It seems unlikely that the fibers comprising the nuclear cortex are chromatin. They lack the characteristic beaded appearance of chromatin strands (Fig. 10) and have a morphology similar to that of fibrous bundles of actin polymers (6). In addition, chromosomes of the oocytes at this stage have contracted and lie in the center of the nucleus at a distance of 100 μm or more from the nuclear envelope (45). Enzymatic treatment of this layer

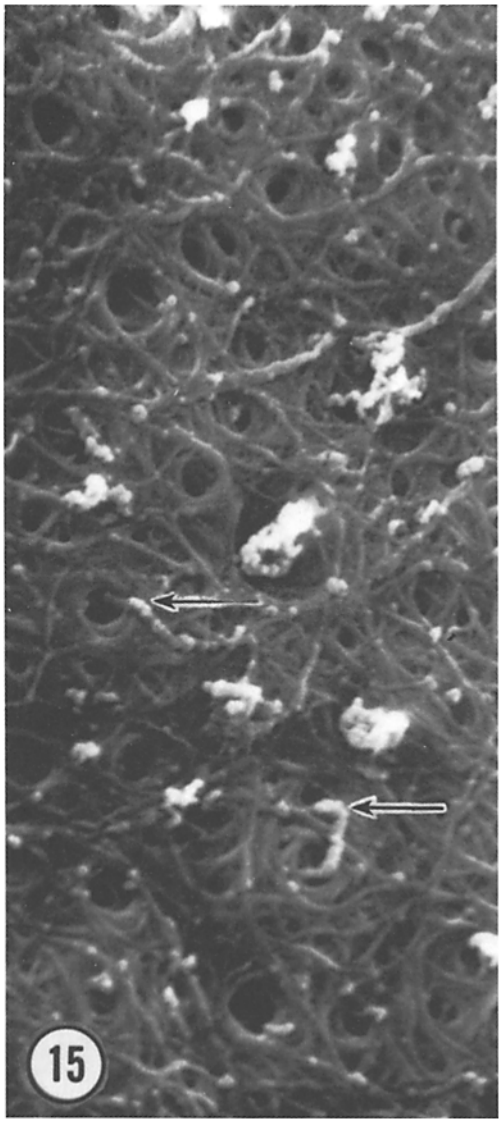

FIGURE 15 The nuclear cortex. The matrix associated with the inner surface of the nuclear envelope is apparent as a series of funnels circumscribed by fibers. This structure is not preserved after isolation, but is seen only after a very rapid fixation. Chains of particles are inserted into the funnels (arrows). × 13,500.

in our hands and by others (46) argues that the layer is proteinaceous, as does high resolution autoradiography (50). The honeycomb layer in amoeba was resolved as 50 Å filaments by Flickinger (14). The fibers remaining after isolation can be extracted with 0.6 M KI, and are approximately of the same diameter as actin polymers observed in the other cells (6). Although there are reports of actin within the nucleus (4, 8, 24, 27, 31) and although a 43,000-dalton band which coelectrophoreses with rabbit muscle actin is found in this nucleus (M. Thoman, unpublished results), it is not possible to rule out the possibility that the actin is cytoplasmic and adhered to the outer surface of the nuclear envelope during the isolation procedure, as discussed by Osborn and Weber (37). Definitive evidence for the presence of actin in the nuclear cortex, such as heavy meromysin decoration, is precluded by the difficulties in isolating this layer intact, and by the problems of fixing actin for the TEM.

If contractile elements can be found within the nucleus, conjectures concerning the motility of the nuclear surface are then possible. The fact that an isolated nuclear matrix has been shown to undergo expansion and contraction in the presence of divalent cations (51) argues for a motile nuclear surface. It then is possible to envision the chains of particles, which are inserted in the intranuclear channels, as material undergoing transport from the nucleus to the cytoplasm. In this work, the image of the nuclear cortex is that of a dynamic structure which is frozen by the very rapid fixation. Perhaps the movements of these particles have been interrupted since the particles appear inserted within the intranuclear channels to varying degrees. These speculations about the active properties of the nuclear surface complex and its role in nucleo-cytoplasmic transport, although tempting, cannot be proven by this work and await further experimentation.

We wish to thank Dr. J. Gerhart for inspiration and encouragement, Dr. Gerhart and Dr. D. Mazia for critically reading this manuscript, and Dr. W. Franke and Dr. G. Maul for valuable discussions.

This research was supported by GM 19363 to J. Gerhart and GM 13882 to D. Mazia. The SEM was purchased for the Electron Microscope Laboratory of the University of California, Berkeley with National Science Foundation (NSF) funds from GM 38-359. The authors wish to thank the Rockefeller Foundation (G. Schatten) and the NSF (M. Thoman) for support. Portions of this work were presented at the First International Congress on Cell Biology, 1976 (43).

Received for publication 4 August 1977, and in revised form 24 January 1978.

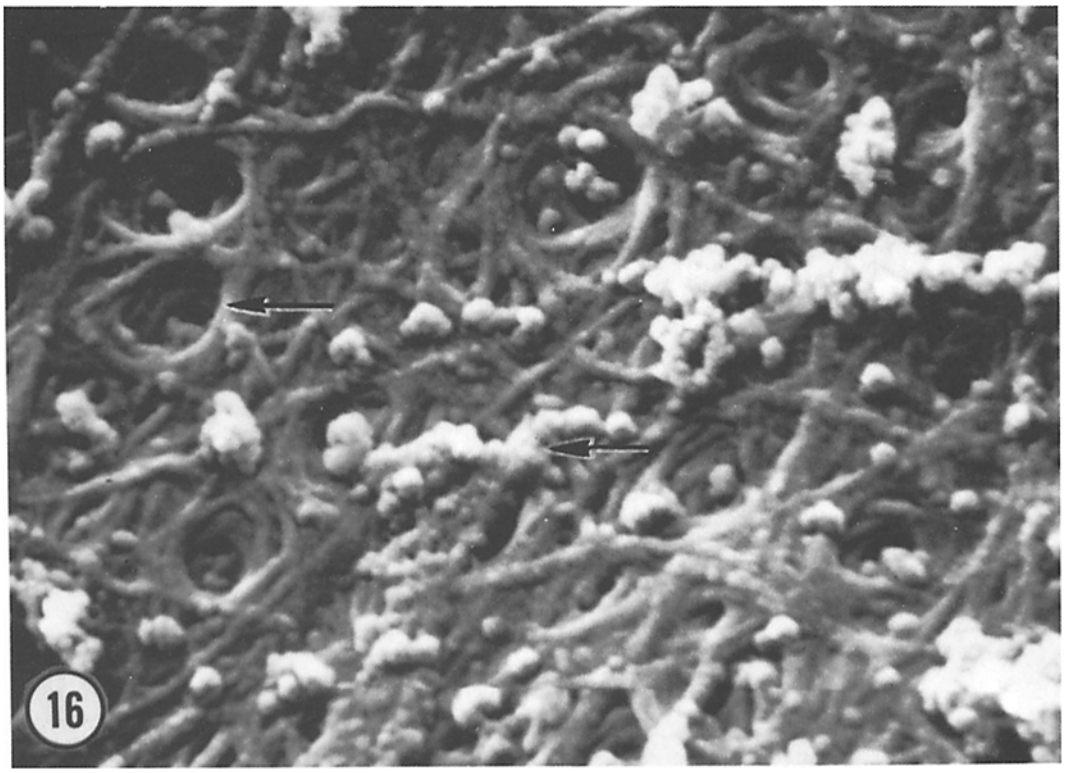

FIGURE 16 The nuclear cortex. This image reveals that the intranuclear channels, which appear as funnels exiting towards the cytoplasm, are composed of overlapping fibers. Particles and chains of particles (arrows) are seen within and associated with the intranuclear channels. × 30,000.

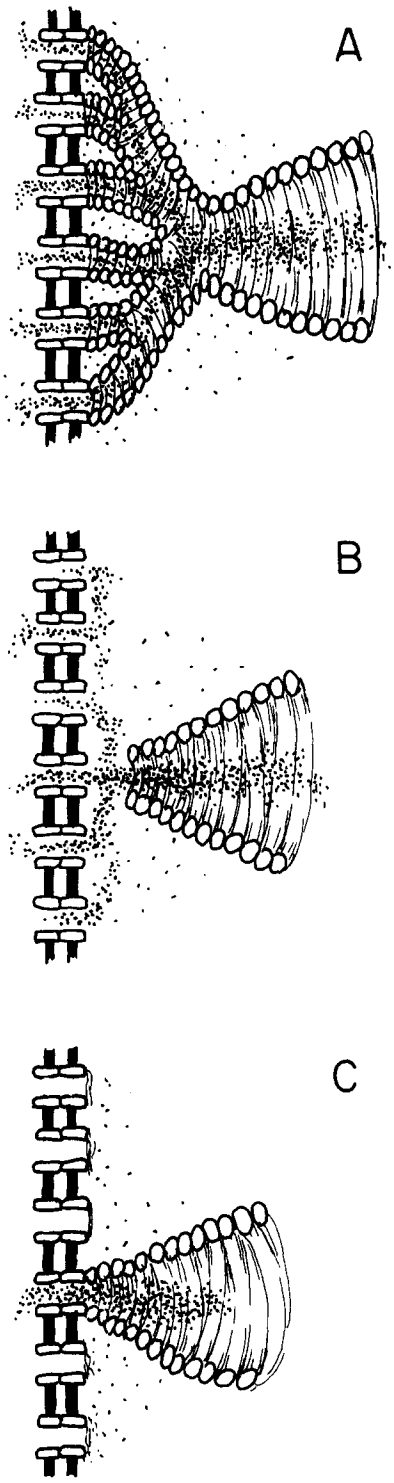

FIGURE 17 Modes of association between the intranuclear channels and the pore complexes. There is a ratio of ~18 nuclear pores per intranuclear channel. If the assumption is made that the nuclear pore complex and the intranuclear channels are involved in nucleo-cytoplasmic transport, then three modes of attachment and transport are possible: (A) The intranuclear channel might bifurcate and service several pores simultaneously. (B) The intranuclear channel might terminate close to, but not at, the pore complex. Material then would sift through several pores. (C) The intranuclear channel might attach to one nuclear pore, and, after some activity, might break that association and immediately reattach to another pore complex.

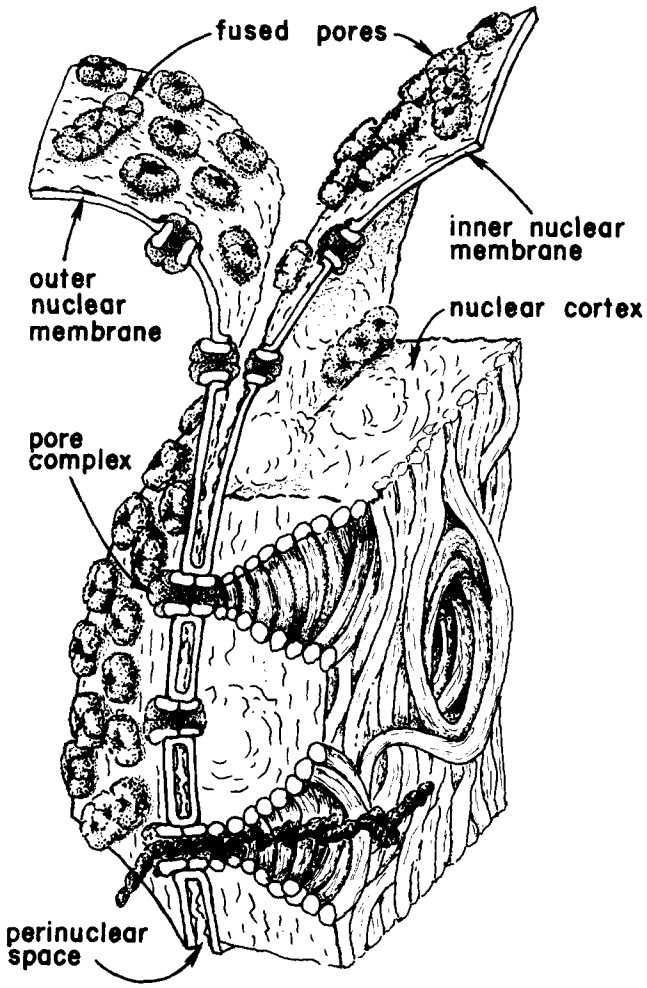

FIGURE 18 The nuclear surface complex. This schematic drawing compiles the data from the four membrane faces and from the nuclear cortex, into an interpretation of the three-dimensional arrangement of the nuclear surface complex. A fuller description appears in the Discussion. The pore complexes appear as tetrameric units, and are often clustered into triplets which share common walls. They can be fractured in the plane of the perinuclear space, resulting in half of the pore complex remaining inserted in the corresponding nuclear membrane; they are never pulled from the membrane. The nuclear cortex appears as a series of overlapping fibers which circumscribe funnels, or intranuclear channels. Material is often found inserted within these intranuclear channels. The association between the nuclear cortex and the pore complex is speculative, and discussed in greater detail in the Discussion and in Fig. 17.

REFERENCES

1. AARONSON, R. P., and G. BLOBEL. 1974. On the attachment of the nuclear pore complex. *J. Cell Biol.* **62:**746–754.
2. BAIRATI, A., and F. E. LEHMANN. 1952. Über die submikroskopische Struktur der Kernmembran bei *Amoeba proteus*. *Experientia (Basel).* **8:**60–61.
3. BEAMS, H. W., T. N. TAHMISIAN, R. DEVINE, and E. ANDERSON. 1975. Ultrastructure of the nuclear membrane of a gregarine parasitic in grasshoppers. *Exp. Cell Res.* **13:**200–204.
4. BLECHER, S. 1975. Actin-like filaments associated with spread chromosomes. *Cytobiologie.* **11:**190–200.
5. CALLAN, H. G., and S. G. TOMLIN. 1950. Experimental studies on amphibian oocyte nuclei. I. Investigation of the structure of the nuclear membrane by means of the electron microscope. *Proc. Roy. Soc. London, Ser. B.* **137:**367–378.
6. CLARKE, M., G. SCHATTEN, D. MAZIA, and J. SPUDICH. 1975. Visualization of actin fibers associ-

ated with the cell membrane in amoebae of *Dictyostelium discoideum*. *Proc. Natl. Acad. Sci. U. S. A.* **72:**1758–1762.

7. Coggeshall, R. E., and D. W. Fawcett. 1964. The fine structure of the central nervous system of the leech *Hirudo medicinalis*. *J. Neurophysiol.* **27:**229–289.
8. Doubas, A., C. Harrington, and J. Bonner. 1975. Major non-histone proteins of rat liver chromatin: Preliminary identification of myosin, actin, tubulin, and tropomyosin. *Proc. Natl. Acad. Sci. U. S. A.* **72:**3902–3906.
9. Engelhardt, P., and K. Pusa. 1972. Nuclear pore complexes: "Press-stud" elements of chromosomes in pairing and control. *Nat. New Biol.* **240:**163–166.
10. Fabergé, A. C. 1974. The nuclear pore complex: Its free existence and an hypothesis as to its origin. *Cell Tissue Res.* **151:**403–415.
11. Fabergé, A. C. 1973. Direct demonstration of eight fold symmetry in nuclear pore. *Z. Zellforsch Mikrosk. Anat.* **136:**183–190.
12. Fawcett, D. W. 1966. On the occurrence of a fibrous lamina on the inner aspect of the nuclear envelope in certain cells of vertebrates. *Am. J. Anat.* **119:**129–146.
13. Feldherr, C. M. 1972. Structure and function of the nuclear envelope. *In* Advances in Cellular and Molecular Biology. E. J. DuPraw, editor. **2:**372–309. Academic Press, Inc., New York.
14. Flickinger, C. J. 1970. The fine structure of the nuclear amoebae: alterations following nuclear transplantation. *Exp. Cell Res.* **60:**225–236.
15. Franke, W. W. 1966. Isolated nuclear membranes. *J. Cell Biol.* **31:**619–623.
16. Franke, W. W., and U. Scheer. 1970. The ultrastructure of the nuclear envelope of amphibian oocytes; a reinvestigation. I. The mature oocyte. *J. Ultrastruct. Res.* **30:**288–316.
17. Franke, W. W., and U. Scheer. 1974. Structure and function of the nuclear envelope. *In* The Nucleus, Vol. 1. H. Busch, editor. Academic Press, Inc., New York. 220–348.
18. Franke, W. W., H. Zentgraf, U. Scheer, and J. Kartenbech. 1973. Membrane linkages at the nuclear envelope. *Cytobiologie* **7:**89–100.
19. Gall, J. G. 1954. Observations on the nuclear membrane with the electron microscope. *Exp. Cell Res.* **7:**197–200.
20. Gall, J. G. 1964. Electron microscopy of the nuclear envelope. *Protoplasmatologia.* **5:**4–25.
21. Gall, J. G. 1967. Octagonal nuclear pores. *J. Cell Biol.* **32:**391–399.
22. Goldstein, L. 1974. Movement of molecules between nucleus and cytoplasm. *In* The Nucleus, Vol. 1. H. Busch, editor. Academic Press, Inc., New York. 388–440.
23. Gray, E. G., and R. W. Guillery. 1963. On nuclear structure in the ventral nerve cord of the nerve cord of *Hirudo medicinalis*. *Z. Zellforsch. Mikrosk. Anat.* **59:**738–745.
24. Hill, R. J., K. Mandrell, and H. Callan. 1974. Nonhistone proteins of the oocyte nucleus of the newt. *J. Cell Sci.* **15:**145–161.
25. Kalifat, S. R., M. Bouteille, and J. Delarue. 1967. Etude ultrastructurale de la lemmelle dense observée en contact de la membrane nucléaire interne. *J. Micros. (Paris).* **6:**1019–1026.
26. Kartenbeck, J., H. Zentgraf, U. Scheer, and W. W. Franke. 1971. The nuclear envelope in freeze etching. *Ergeb. Anat. Entwicklungsgesch.* **45:**1–55.
27. Kashnig, D. M., and C. B. Kasper. 1969. Isolation, morphology and composition of the nuclear membrane for from rat liver. *J. Biol. Chem.* **244:**3786–3792.
28. Kasper, C. B. 1974. Chemical and biochemical properties of the nuclear envelope. *In* The Nucleus, Vol. 1. H. Busch, editor. Academic Press, Inc., New York. 349–387.
29. Kirschner, R. H., M. Rusli, and T. E. Martin. 1977. Characterization of the nuclear envelope, pore complex, and dense lamina of mouse liver nuclei by high resolution scanning electron microscope. *J. Cell Biol.* **72:**118–132.
30. Loewenstein, W. R. 1964. Permeability of the nuclear membrane as determined with electrical methods. *Protoplasmatologia.* **5:**26–34.
31. Maundrell, K. 1975. Proteins of the newt oocyte nucleus: Analysis of the nonhistone proteins from lampbrush chromosomes, nucleoli and nuclear sap. *J. Cell Sci.* **17:**579–588.
32. Maul, G. G. 1971. On the octagonality of the nuclear pore complex. *J. Cell Biol.* **51:**558–563.
33. Maul, G. G. The nuclear and cytoplasmic pore complex: structure, dynamics, distribution. *Int. Rev. Cytol.* In press.
34. Maul, G. G., H. M. Maul, T. E. Scogna, M. W. Lieberman, G. S. Stein, B. Y. Hsu, and T. W. Borun. 1972. Time sequence of nuclear pore formation in phytohemagglutinin-stimulated lymphocytes and in HeLa cells during the cell cycle. *J. Cell Biol.* **55:**433–447.
35. Mazanec, K. 1967. Presence de la "zonula nucleum limitans" dans quelques cellules humaines. *J. Micros. (Paris).* **6:**1027–1032.
36. Mazia, D., G. Schatten, and W. Sale. 1975. Adhesion of cells to surface coated with polylysine; applications to electron microscopy. *J. Cell Biol.* **64:**198–200.
37. Osborn, M., and K. Weber. 1977. The detergent-resistant cytoskeleton of tissue culture cells includes the nucleus and the microfilament bundles. *Exp. Cell Res.* **106:**339–350.
38. Pappas, G. D. 1956. The fine structure of the nuclear envelope of *Amoeba proteus*. *J. Biophys.*

Biochem. Cytol. **3** (Suppl.):431–433.

39. PATRIZI, G. 1968. Further consideration on the ultrastructure of the nuclear periphery with observation on human plasma cells. *J. Microsc. (Paris).* **7**:293–296.
40. PATRIZI, G., and M. POGER. 1967. The ultrastructure of the nuclear periphery: The zonula nucleum limitans. *J. Ultrastruct. Res.* **17**:127–136.
41. POLLISTER, A. W., M. GETTNER, and R. WARD. 1954. Nucleocytoplasmic interchange in oocytes. *Science (Wash. D. C.).* **120**:789.
42. SCHATTEN, G., and D. MAZIA. 1976. The penetration of the spermatozoon through the sea urchin egg at fertilization; observations from the outside on whole egg and from inside on isolated surfaces. *Exp. Cell Res.* **98**:325–337.
43. SCHATTEN, G., M. THOMAN, and J. GERHART. 1976. The nuclear envelope as observed with the scanning electron microscope. *J. Cell Biol.* **70** (2, Pt. 2):40*a*. (Abstr.).
44. SCHEER, U., J. KARTENBECK, M. F. TRENDELENBURG, J. STADLER, and W. W. FRANKE. 1976. Experimental disintegration of the nuclear envelope: Evidence for pore connecting fibrils. *J. Cell Biol.* **69**:1–18.
45. SCHEER, U. 1970. The ultrastructure of the nuclear envelope of Amphibian oocytes: A Reinvestigation. *J. Cell Biol.* **45**:445–449.
46. STELLY, N., B. J. STEVENS, and J. ANDRE. 1970. Etude cytolchimique de la lamelle dense de l'enveloppe nucleaire. *J. Microsc. (Paris).* **9**:1015–1028.
47. STEVENS, B. J., and J. ANDRE. 1969. The nuclear envelope. *In* Handbook of Molecular Cytology, A. Lima-de-Faria, editor. North-Holland Publishing Co., Amsterdam. 837–871.
48. VACQUIER, V. 1975. The isolation of intact cortical granules from sea urchin eggs: calcium ions trigger granules discharge. *Dev. Biol.* **43**:62–74.
49. WATSON, M. L. 1959. Further observations on the nuclear envelope of the animal cell. *J. Biophys. Biochem. Cytol.* **6**:147–156.
50. WISE, C. G., A. R. STEVENS, and D. M. PRESCOTT. 1972. Evidence of RNA in helices of *Amoeba proteus*. *Exp. Cell Res.* **75**:347–352.
51. WUNDERLICH, W., and G. HERLAN. 1977. A reversibly contractile nuclear matrix: its isolation, structure and composition. *J. Cell Biol.* **73**:271–278.